Low Dimensional Materials: Syntheses, Structures, and Optical Properties of Rb_2CuTaS_4, $Rb_2CuTaSe_4$, $RbCu_2TaSe_4$, $K_3Ag_3Ta_2Se_8$, and $Rb_3AgTa_2Se_{12}$

Yuandong Wu, Christian Näther, and Wolfgang Bensch

Institut für Anorganische Chemie, Christian-Albrechts-Universität Kiel, Olshausenstraße 40, D-24098 Kiel, Germany

Reprint requests to Prof. Dr. W. Bensch. Fax: +49-(0)431-880-1520.
E-mail: wbensch@ac.uni-kiel.de

Z. Naturforsch. **59b,** 1006 – 1014 (2004); received July 14, 2004

Dedicated to Professor Kurt O. Klepp on the occasion of his 60th birthday

The new compounds Rb_2CuTaS_4 (**1**), $Rb_2CuTaSe_4$ (**2**), $RbCu_2TaSe_4$ (**3**), $K_3Ag_3Ta_2Se_8$ (**4**), and $Rb_3AgTa_2Se_{12}$ (**5**) have been synthesized by the reactive flux method at 773 or 873 K. Their crystal structures were determined by single crystal X-ray diffraction. Crystal data for **1**: space group *Fddd*, $a = 5.598(1)$, $b = 13.512(4)$, $c = 23.854(5)$ Å, $Z = 8$; Crystal data for **2**: space group *Fddd*, $a = 5.782(1)$, $b = 13.924(3)$, $c = 24.653(5)$ Å, $Z = 8$; Crystal data for **3**: space group $C2cm$, $a = 5.7218(3)$, $b = 19.2463(13)$, $c = 7.7456(5)$ Å, $Z = 4$; Crystal data for **4**: space group $C2/c$, $a = 25.1374(19)$, $b = 6.1007(3)$, $c = 14.4030(11)$ Å, $\beta = 119.703(8)^\circ$, $Z = 4$; Crystal data for **5**: space group $P2_1/n$, $a = 9.8186(6)$, $b = 13.7462(11)$, $c = 15.7368(9)$ Å, $\beta = 96.681(7)^\circ$, $Z = 4$. The compounds **1** and **2** are built up of $^1_\infty[CuTaQ_4]^{2-}$ anionic chains which are formed by edge-sharing CuQ_4 and TaQ_4 tetrahedra. The rubidium cations are located between the chains. Compound **3** consists of $^2_\infty[Cu_2TaSe_4]^-$ anionic layers separated by rubidium cations. The anionic layers are formed by $^1_\infty[CuTaSe_4]^{2-}$ chains which are connected by $CuSe_4$ tetrahedra that share common edges with the $TaSe_4$ tetrahedra of neighboring chains. In compound **4** $^1_\infty[Ag_3Ta_2Se_8]^{3-}$ anionic chains are found which are separated by potassium cations. These chains are formed by successive corner sharing of $AgSe_4$ tetrahedra and edge sharing between $AgSe_4$ and $TaSe_4$ tetrahedra. All three structures are closely related with the sulvanite (Cu_3VS_4) structure type. Compound **5** contains a one dimensional $^1_\infty[AgTa_2Se_{12}]^{3-}$ anionic chain formed by interconnection of $AgSe_4$ tetrahedra and $[Ta_2Se_{11}]$ units. In the structure three monoselenide, three diselenide, and one triselenide anions are found. Raman and far-IR spectroscopic data of compounds **1** and **4** were collected and an interpretation is presented.

Key words: Tantalum Compound, Quaternary Chalcogenides, Crystal Structures, Flux Reaction, Optical Properties

Introduction

Low-dimensional compounds exhibit many interesting physical properties such as high temperature superconductivity, the formation of charge density waves, and low-dimensional magnetism. In these compounds either two-dimensional slabs are stacked along a crystallographic direction or chains are in a juxtaposition. Within the slabs or chains ionic, covalent, or metallic interactions dominate. Between them very often only weak interactions such as van der Waals forces occur or they are separated by alkaline or alkaline earth cations. The quaternary alkali metal group 5 metal chalcogenides with compositions $A_2M^IM^VQ_4$ (A = K, Rb, Cs; M^I = Cu, Ag; M^V = V, Nb, Ta; Q = S, Se) [1 – 9], $ACu_2M^VQ_4$ (A = K, Rb, Cs; M^V = V, Nb, Ta; Q = S, Se, Te) [10 – 18], $K_3Cu_3M^V{}_2Q_8$ (M^V = Nb, Ta; Q = S, Se) [19], and $K_3CuNb_2Se_{12}$ [20] crystallize with low-dimensional anionic building units. The structures of these compounds except $K_3CuNb_2Se_{12}$ can be derived from the sulvanite (Cu_3VS_4) type. Sequential substitution of A = K, Rb, Cs for Cu ions results in a decrease of the dimensionality of the structures, from the three-dimensional covalent network in Cu_3VS_4 *via* two-dimensional metal chalcogen layers in $ACu_2M^VQ_4$, to infinite one-dimensional metal-chalcogen chains in

Compound	**1**	**2**	**3**	**4**	**5**
Formula	Rb_2CuTaS_4	$Rb_2CuTaSe_4$	$RbCu_2TaSe_4$	$K_3Ag_3Ta_2Se_8$	$Rb_3AgTa_2Se_{12}$
Crystal system	orthorhombic	orthorhombic	orthorhombic	monoclinic	monoclinic
Space group	*Fddd*	*Fddd*	*C2cm*	$C2/c$	$P2_1/n$
a [Å]	5.598(1)	5.7820(5)	5.7218(3)	25.1374(19)	9.8186(6)
b [Å]	13.512(4)	13.9240(12)	19.2463(13)	6.1007(3)	13.7462(11)
c [Å]	23.854(5)	24.6526(29)	7.7456(5)	14.4030(11)	15.7368(9)
β [°]	90	90	90	119.703(8)	96.681(7)
V [Å^3]	1804.2(7)	1984.7(7)	852.97(9)	1918.6(2)	2109.5(2)
Z	8	8	4	4	4
T [K]	293	293	293	293	293
calcd. den. (g.cm^{-3})	4.003	4.895	5.524	4.966	5.270
μ [mm^{-1}]	26.031	37.494	40.376	30.171	38.829
$F(000)$	1920	2496	1216	2464	4852
2θ Range [°]	$6° \le 2\theta \le 60°$	$7° \le 2\theta \le 56°$	$5° \le 2\theta \le 56°$	$6° \le 2\theta \le 56°$	$5° \le 2\theta \le 56°$
Index range	$-1 \le h \le 5$	$-7 \le h \le 7$	$-7 \le h \le 7$	$-32 \le h \le 32$	$-7 \le h \le 7$
	$-1 \le k \le 18$	$-18 \le k \le 17$	$-25 \le k \le 25$	$-7 \le k \le 7$	$-25 \le k \le 25$
	$-1 \le l \le 33$	$-33 \le l \le 32$	$-10 \le l \le 10$	$-18 \le l \le 19$	$-10 \le l \le 10$
Indep. refl.	585	597	1113	2291	4852
refl. [$F_o > 4\sigma(F_o)$]	481	488	1036	2059	4164
R_{int}	0.0242	0.0614	0.0544	0.0407	0.0548
Min/max. transm.	0.1727/0.3345	0.0549/0.1746	0.0115/0.0581	0.0438/0.2464	0.0097/0.0846
No. parameters	22	22	47	76	164
w^*	0.0177	0.0408	0.0455	0.0778	0.0370
$R1$ for $F_o > 4\sigma(F_o)$	0.0186	0.0259	0.0272	0.0381	0.0274
$wR2$ for all data	0.0520	0.0657	0.0687	0.1016	0.0658
GooF	1.190	1.049	1.051	1.041	1.025
BASF	–	–	0.259	–	–
$\Delta\rho$[eÅ^{-3}]	0.998/−0.938	1.274/−2.361	1.285/−2.591	2.665/−3.067	1.361/−1.771

Table 1. Technical details of data acquisition and refinements.

* $w = 1/[\sigma^2({F_o}^2) + (x \cdot P)^2 + y \cdot P]$; $P = (\mathrm{Max}({F_o}^2) + 2 \cdot {F_c}^2)/3$.

$A_2M^{I}M^{V}Q_4$ and $K_3Cu_3M^{V}{}_2Q_8$, and finally to isolated MQ_4 ions in A_3MQ_4. This series of compounds obviously shows the influence of the size and distinct bonding nature of the cations onto the dimensionality of the structures. $K_3CuNb_2Se_{12}$ is another example containing a one-dimensional bimetallic chain which comprises $CuSe_4$ tetrahedra and $[Nb_2Se_{11}]$ units with each Nb atom in a pentagonal bipyramidal environment. Here we describe the syntheses and structures of the five quaternary alkali metal-group 5 chalcogenides, Rb_2CuTaS_4, $Rb_2CuTaSe_4$, $RbCu_2TaSe_4$, $K_3Ag_3Ta_2Se_8$, and $Rb_3AgTa_2Se_{12}$. In addition, we draw some simple connections between the different formulations of the quaternary alkali metal group 5 chalcogenides.

Experimental Section

Syntheses

The following reagents were commercially available: K (Strem, 99.95%), Rb (Strem, 99+%), Cu (alfa, 99.5%), Ag (Degussa, 99.5%), Ta (Strem, 99.98%), S (Heraeus, 99.99%), Se (Riedel-De Haën, 99.5%), Te (Retorte, 99.999%). The chalcogenides A_2Q_3 (A = K, Rb; Q = Se, Te) were synthesized from reactions of stoichiometric amounts of elemental A and Q dissolved in liquid ammonia under an argon atmosphere. The tantalum powder was activated with ultrasonic radiation in dry acetone.

*Rb_2CuTaS_4 (**1**):* The starting materials Rb_2Te_3, Cu, Ta, and S in a 2:1:1:12 molar ratio were thoroughly mixed and loaded into a Pyrex tube in a nitrogen glove box. The tube was evacuated and flame sealed at the pressure of $\sim 10^{-3}$ mbar. The mixture was heated at 773 K for 5 days, followed by cooling to 373 K at a rate of 3 K/h and the furnace was turned off. The product was washed with DMF to remove excess rubidium sulfides and dried with anhydrous acetone. It contained transparent colorless needles (yield: about 90% based on Ta) and black needles of tellurium. The product is stable under dry air for several months.

*$Rb_2CuTaSe_4$ (**2**):* The preparation and isolation of **2** were similar to those of **1**. However, the mixture of Rb_2Se_3, Cu, Ta, Se in a molar ratio of 4:1:1:8 was heated at 873 K for 5 days in a fused silica tube. After cooling the mixture with 3 K/h, transparent amber-colored platelet crystals were obtained in a yield of about 100%. The compound is stable in dry air for several weeks. The homogeneity of the product was confirmed by comparison of the experimental and calculated X-ray diffraction powder patterns.

*$RbCu_2TaSe_4$ (**3**):* The procedure for the preparation of **3** is the same as that for **2** except that the molar ratio Rb_2Se_3, Cu, Ta, Se was changed to 3:6:4:7. The product contained transparent yellow platelet crystals in a 80% yield. The crystals

Table 2. Atomic coordinates and equivalent isotropic displacement parameters U_{eq} ($Å^2 \cdot 10^3$). Estimated standards deviations are given in parentheses. The U_{eq} is defined as one third of the trace of the orthogonalized U_{ij} tensor.

	x	*y*	*z*	U_{eq}
Rb_2CuTaS_4:				
Ta	1/8	1/8	5/8	13(1)
Cu	1/8	1/8	1/8	23(1)
Se	0.3629(3)	0.7224(1)	0.1794(1)	28(1)
Rb	1/8	1/8	0.4472(1)	28(1)
$Rb_2CuTaSe_4$:				
Ta	1/8	1/8	5/8	11(1)
Cu	1/8	1/8	1/8	21(1)
Se	0.3662(1)	0.7249(1)	0.1810(1)	20(1)
Rb	1/8	1/8	0.4462(1)	26(1)
$RbCu_2TaSe_4$:				
Ta(1)	0.5444(1)	0.1086(1)	1/4	16(1)
Cu(1)	0.0436(6)	0.1062(1)	1/4	25(1)
Cu(2)	0.5649(4)	0	0	25(1)
Se(1)	0.2972(2)	0.2090(1)	1/4	32(1)
Se(2)	0.2995(2)	0.0039(1)	1/4	19(1)
Se(3)	0.7898(2)	0.1079(1)	0.9955(1)	24(1)
Rb(1)	0.7975(2)	0.3171(1)	1/4	37(1)
$K_3Ag_3Ta_2Se_8$:				
Ta(1)	0.1292(1)	0.6945(1)	0.2823(1)	8(1)
Ag(1)	0	0.6909(1)	1/4	21(1)
Ag(2)	0.1290(1)	0.1946(1)	0.2927(1)	20(1)
Se(1)	0.1598(1)	0.9255(1)	0.1812(1)	16(1)
Se(2)	0.0464(1)	0.4699(1)	0.1489(1)	16(1)
Se(3)	0.2171(1)	0.4809(1)	0.3995(1)	15(1)
K(1)	0.1944(1)	0.4266(1)	0.1074(1)	24(1)
K(2)	0	0	0	22(1)
$Rb_3AgTa_2Se_{12}$:				
Ta(1)	0.1575(1)	0.2784(1)	0.0802(1)	14(1)
Ta(2)	−0.0149(1)	0.2215(1)	0.2712(1)	14(1)
Ag(1)	−0.1989(1)	0.1723(1)	0.4187(1)	28(1)
Rb(1)	−0.0067(1)	−0.1059(1)	0.1590(1)	34(1)
Rb(2)	0.5694(1)	0.0843(1)	0.2222(1)	33(1)
Rb(3)	−0.2240(1)	−0.0850(1)	0.4927(1)	33(1)
Se(1)	0.1966(1)	0.2793(1)	0.3669(1)	25(1)
Se(2)	0.2354(1)	0.1836(1)	0.2456(1)	21(1)
Se(3)	−0.0706(1)	0.0618(1)	0.3254(1)	22(1)
Se(4)	0.4251(1)	0.2704(1)	0.0736(1)	22(1)
Se(5)	0.0240(1)	0.3892(1)	0.1729(1)	18(1)
Se(6)	−0.1339(1)	0.3525(1)	0.3612(1)	23(1)
Se(7)	−0.2401(1)	0.2863(1)	0.1958(1)	23(1)
Se(8)	0.2585(1)	0.4301(1)	0.1626(1)	22(1)
Se(9)	−0.0495(1)	0.1613(1)	0.1041(1)	22(1)
Se(10)	0.0509(1)	0.3421(1)	−0.0549(1)	23(1)
Se(11)	0.1614(1)	0.0933(1)	0.0611(1)	26(1)
Se(12)	0.4932(1)	0.1252(1)	0.0052(1)	34(1)

are stable in dry air for several weeks. The homogeneity of the product was confirmed through X-ray powder diffraction.

*$K_3Ag_3Ta_2Se_8$ (**4**):* Crystals were prepared reacting a mixture of K_2Se_3, Ag, Ta, and Se with a molar ratio of 3:6:4:7. After being sealed in a silica tube under vacuum, the starting material was heated to 773 K, held there for 24 h, then ramped to 973 K, kept there for 4 days, and cooled down to 373 K at a rate of 3 K/h. After removing excess K_2Se_x flux, crystals suitable for X-ray diffraction studies were picked out manually from the mixture of transparent yellow needles ($\sim$ 70% yield based on Ta) and black needles, which have not yet been identified.

Table 3. Selected bond lengths (Å) for Rb_2CuTaS_4 (**1**) and $Rb_2CuTaSe_4$ (**2**).

	Rb_2CuTaS_4	*$Rb_2CuTaSe_4$*
Ta - Q ×4	2.278(1)	2.405(1)
Cu - Q ×4	2.360(1)	2.465(1)
Rb - Q ×2	3.448(2)	3.547(1)
Rb - Q ×2	3.490(2)	3.611(1)
Rb - Q ×2	3.557(2)	3.629(1)
Rb - Q ×2	3.656(2)	3.770(1)

Table 4. Selected bond lengths (Å) for $RbCu_2TaSe_4$ (**3**).

Ta(1)	-	Se(1)	2.395(2)	Ta(1)	-	Se(3) ×2	2.420(1)
Ta(1)	-	Se(2)	2.454(1)	Cu(1)	-	Se(1)	2.454(3)
Cu(1)	-	Se(2)	2.453(3)	Cu(1)	-	Se(3) ×2	2.448(2)
Cu(2)	-	Se(2) ×2	2.462(2)	Cu(2)	-	Se(3) ×2	2.443(2)
Rb(1)	-	Se(1)	3.537(2)	Rb(1)	-	Se(2)	3.596(2)
Rb(1)	-	Se(3) ×2	3.693(2)	Rb(1)	-	Se(3) ×2	3.760(2)
Rb(1)	-	Se(1) ×2	3.905(1)				

*$Rb_3AgTa_2Se_{12}$ (**5**):* Compound **5** can be obtained under the same reaction conditions used for **2** but with more selenium (molar ratio: Rb_2Se_3: Ag: Ta: Se = 3:2:4:15). The product was isolated by removing the excess Rb_2Se_x flux with DMF followed by washing with acetone. The product consists of black chunk crystals (yield: 90% based on Ta) which are insoluble in water and stable in air. The by-product consisting of transparent amber-colored platelet crystals was identified as $RbAg_2TaSe_4$ by comparison of the calculated and experimental powder patterns.

Single crystal X-ray diffraction

Single crystal investigation of compound **1** was performed using a Philips PW1100 4-circle diffractometer, and of compounds **2 – 5** using an Imaging Plate Diffraction System (IPDS) with monochromated Mo-K_α-radiation (λ = 0.71073 Å). The intensities were treated in the normal way applying Lorentz and polarization correction. For compound **1** an empirical absorption correction based on ψ-scan reflections and for compounds **2 – 5** face indexed absorption corrections were applied.

All structures were solved with direct methods using SHELXS-97 and refined against F_o^2 using SHELXL-97 [21]. All atoms were refined with anisotropic displacement parameters. The crystal of compound **3** was racemically twinned and therefore, a twin refinement using SHELXL-97 was performed (BASF parameter: 0.26(3)). In order to compare the structure of **3** with that of KCu_2MSe_4 (M = Nb, Ta)

Table 5. Selected bond lengths (Å) for $K_3Ag_3Ta_2Se_8$ (**4**).

Ta(1)	-	Se(1)	2.410(1)	Ta(1)	-	Se(2)	2.437(1)
Ta(1)	-	Se(3)	2.395(1)	Ta(1)	-	Se(4)	2.447(1)
Ag(1)	-	Se(2) ×2	2.642(1)	Ag(1)	-	Se(4) ×2	2.650(1)
Ag(2)	-	Se(1)	2.667(1)	Ag(2)	-	Se(2)	2.676(1)
Ag(2)	-	Se(3)	2.636(1)	Ag(2)	-	Se(4)	2.629(1)
K(1)	-	Se(1)	3.414(2)	K(1)	-	Se(1)	3.485(2)
K(1)	-	Se(3)	3.363(2)	K(1)	-	Se(3)	3.546(2)
K(1)	-	Se(4)	3.466(2)	K(2)	-	Se(1) ×2	3.572(1)
K(2)	-	Se(2)	3.420(1)	K(2)	-	Se(2) ×2	3.733(1)
K(2)	-	Se(4) ×2	3.556(1)				

Table 6. Selected bond lengths (Å) for $Rb_3AgTa_2Se_{12}$ (**5**).

Ta(1)	-	Se(2)	2.931(1)	Ta(1)	-	Se(4)	2.643(1)
Ta(1)	-	Se(5)	2.572(1)	Ta(1)	-	Se(8)	2.591(1)
Ta(1)	-	Se(9)	2.654(1)	Ta(1)	-	Se(10)	2.421(1)
Ta(1)	-	Se(11)	2.563(1)	Ta(2)	-	Se(1)	2.547(1)
Ta(2)	-	Se(2)	2.588(1)	Ta(2)	-	Se(3)	2.440(1)
Ta(2)	-	Se(5)	2.827(1)	Ta(2)	-	Se(6)	2.646(1)
Ta(2)	-	Se(7)	2.546(1)	Ta(2)	-	Se(9)	2.740(1)
Ag(1)	-	Se(3)	2.546(1)	Ag(1)	-	Se(4)	2.712(1)
Ag(1)	-	Se(6)	2.737(1)	Ag(1)	-	Se(10)	2.547(1)
Rb(1)	-	Se(1)	3.495(1)	Rb(1)	-	Se(3)	3.598(1)
Rb(1)	-	Se(6)	3.552(1)	Rb(1)	-	Se(7)	3.862(1)
Rb(1)	-	Se(8)	3.532(1)	Rb(1)	-	Se(9)	3.785(1)
Rb(1)	-	Se(10)	3.640(1)	Rb(1)	-	Se(11)	3.620(1)
Rb(1)	-	Se(11)	3.631(1)	Rb(2)	-	Se(2)	3.611(1)
Rb(2)	-	Se(3)	3.727(1)	Rb(2)	-	Se(4)	3.639(1)
Rb(2)	-	Se(5)	3.334(1)	Rb(2)	-	Se(6)	3.532(1)
Rb(2)	-	Se(7)	3.400(1)	Rb(2)	-	Se(10)	3.676(1)
Rb(2)	-	Se(12)	3.456(1)	Rb(3)	-	Se(1)	3.456(1)
Rb(3)	-	Se(3)	3.768(1)	Rb(3)	-	Se(3)	3.839(1)
Rb(3)	-	Se(4)	3.791(1)	Rb(3)	-	Se(5)	3.716(1)
Rb(3)	-	Se(7)	3.437(1)	Rb(3)	-	Se(8)	3.438(1)
Rb(3)	-	Se(10)	3.604(1)				

[13, 15, 16] directly, **3** was refined in the non-conventional setting (*C*2*cm*) of space group *Ama*2. With the matrix (0 0 −1 0 1 0 1 0 0) the conventional setting *Ama*2 is achieved. Technical details of the data acquisition as well as some refinement results are summarized in Table 1. Atomic coordinates as well as equivalent isotropic displacement parameters are listed in Table 2. Selected bond lengths are given in Tables 3 – 6.

Further details of the crystal structure investigation can be ordered referring to the No CSD-414271 (Rb_2CuTaS_4), CSD-414272 ($Rb_2CuTaSe_4$), CSD-414274 ($RbCu_2TaSe_4$), CSD-414270 ($K_3Ag_3Ta_2Se_8$), and CSD-414273 ($Rb_3AgTa_2Se_{12}$), the authors and the citation of this paper at the Fachinformationszentrum Karlsruhe, Gesellschaft für wissenschaftlich-technische Information mbH. D-76344 Eggenstein-Leopoldshafen (Germany). E-mail: crysdata@fiz-karlsruhe.de.

Infrared and Raman spectroscopy

FIR spectra were recorded between 80 and 550 cm^{-1} (resolution = 2 cm^{-1}) on an ISF-66 device (Bruker) with

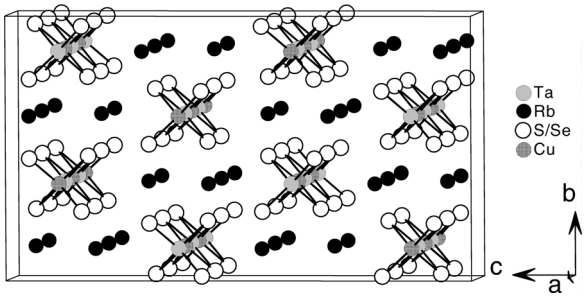

Fig. 1. View of the Rb_2CuTaQ_4 structure (Q = S (**1**), Se (**2**)) approximately along the *a* axis.

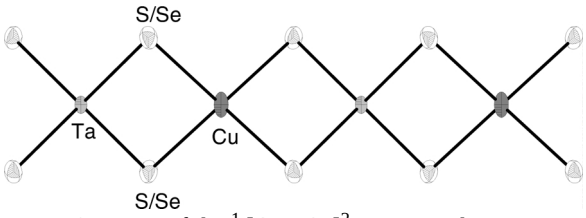

Fig. 2. Structure of the $^1_\infty[CuTaQ_4]^{2-}$ anionic chain in compounds **1** and **2**. Displacement ellipsoids are drawn at the 50% probability level.

compounds **1** and **4** pressed in polyethylene pellets. The FT-Raman spectrum was measured on an ISF-66 spectrometer (Bruker) with an additional FRA 106 Raman modul. A Nd/YAG laser was used as source for excitation (λ = 1064 nm). The samples were prepared on Al-sample holders. The measuring range was 100 to 3500 cm^{-1} with a resolution of 2 cm^{-1}.

Results and Discussions

Structures

The structures of the isostructural compounds Rb_2CuTaS_4 (**1**) and $Rb_2CuTaSe_4$ (**2**) are shown in Fig. 1. They consist of infinite $^1_\infty[CuTaQ_4]^{2-}$ chains running parallel to [100] which are separated by Rb^+ ions. These chains are illustrated in Fig. 2. Within the chains the Cu and Ta atoms are in a tetrahedral coordination of four Q atoms. These tetrahedra share two opposite edges, and CuQ_4 and TaQ_4 tetrahedra alternate along the chain. The Cu and Ta atoms have crystallographically imposed 222 site symmetry. Consequently, each atom must have single M – Q distances and each can have three independent Q – M – Q angles. The Cu – Q distances and Ta – Q distances are 2.360(1) Å (Cu – S), 2.278(1) Å (Ta – S) in **1** and 2.465(1) Å (Cu – Se), 2.405(1) Å (Ta – Se) in **2**. The Q – Ta – Q angles are 108.45(7)°, 109.38(7)°,

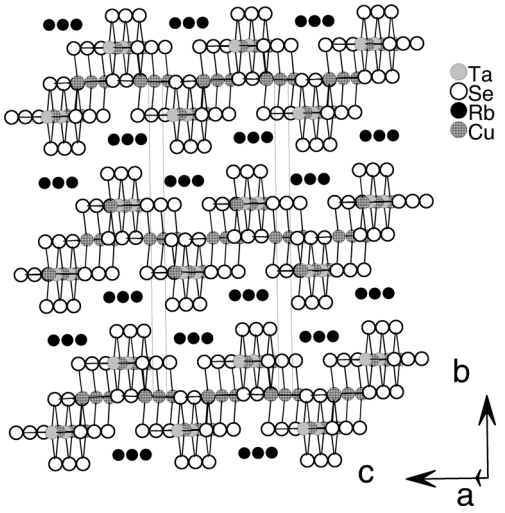

Fig. 3. Crystal structure of $RbCu_2TaSe_4$ (**3**) with view approximately along [100].

and 110.60(7)° in **1** and 109.11(3)°, 109.35(3)° and 109.95(3)° in **2**. The S – Cu – S angles are 103.09(7)°, 112.18(7)°, and 113.33(7)° in **1** and the Se – Cu – Se angles are 105.26(3)°, 111.91(3)°, and 113.33(3)° in **2**, indicating distortions of the MQ_4 tetrahedra which are more pronounced for M = Cu. The shortest interchain Q – Q distances of 3.778(1) Å (S – S) in compound **1** and 3.803(1) Å (Se – Se) in compound **2** are slightly longer the sum of the van der Waals radii (3.6 Å for S; 3.8 Å for Se). Therefore, there are no interactions between the anionic chains in these compounds. The Rb^+ ions are coordinated by eight S (Se) atoms that belong to three different anionic chains. The Rb – S distances range from 3.448(2) to 3.656(2) Å (average: 3.538(2) Å) and the Rb – Se distances are between 3.547(1) and 3.770(1) Å (average: 3.639(1) Å). These distances agree well with those found in the isostructural compounds $A_2M^IM^VQ_4$ (A = K, Rb, Cs; M^I = Cu, Ag; M^V = V, Nb, Ta; Q = S, Se) [1 – 9]. Due to the long Q – Q distances there are no significant interactions. The formal oxidation states Rb(+1), Cu(+1), Ta(+5), and S(-2)/Se(-2) can be assigned.

The structure of $RbCu_2TaSe_4$ (**3**) is shown in Fig. 3. It is composed of two-dimensional $[Cu_2TaSe_4]^-$ layers which are parallel to the (010) plane (Fig. 4) and Rb^+ ions located between the layers. The shortest interlayer Se – Se distance of 4.006(1) Å is longer than the sum of the van der Waals radii of Se. Obviously there are no interactions between the adjacent layers. Within the $[Cu_2TaSe_4]^-$ layers Ta and Cu atoms

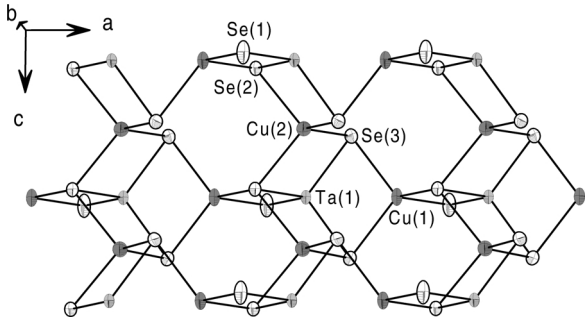

Fig. 4. Structure of the $^2_\infty[Cu_2TaSe_4]^{1-}$ layer in compound **3** with atomic labeling. Displacement ellipsoids are drawn at the 50% probability level.

are tetrahedrally coordinated by Se atoms. The $TaSe_4$ and $Cu(1)Se_4$ tetrahedra are sharing common edges to form $[Cu(1)TaSe_4]$ chains along [100], like in the one-dimensional chains in $Rb_2CuTaSe_4$. The $Cu(2)Se_4$ tetrahedra share common corners with $Cu(1)Se_4$ tetrahedra along [100] and have a common edge with $TaSe_4$ tetrahedra along [001]. This connection mode yields the $[Cu_2TaSe_4]^-$ layers. The Ta – Se bond lengths range from 2.395(2) to 2.454(1) Å, matching well with those in $Rb_2CuTaSe_4$ (**2**). The Se – Ta – Se angles vary from 109.07(6)° to 110.31(3)°, close to the normal tetrahedral values. The Cu – Se bonds from 2.443(2) to 2.462(2) Å are slightly shorter than the Cu – Se distance (2.465(1) Å) in $Rb_2CuTaSe_4$ (**2**). The Se – Cu – Se angles about the two crystallographically independent Cu atoms are different. The Se – Cu(1) – Se angles are close to the normal tetrahedral value (107.1(1)° – 111.39(5)°), while the Se – Cu(2) – Se angles scatter from 103.8(1)° to 116.4(1)°, which clearly indicates the stronger distortion of the $Cu(2)Se_4$ tetrahedron. The Rb^+ ions are coordinated by nine Se atoms choosing a cutoff of 4.0 Å for the Rb – Se distances. The Rb-Se bond lengths range from 3.537(2) to 3.905(3) Å (average: 3.698(2) Å). The geometry around Rb^+ is similar to that of K^+ in KCu_2MSe_4 (M = Nb, Ta) [13, 16, 17] which is a slightly distorted tricapped trigonal prism, unlike the highly distorted trigonal prism of the Cs cations in $CsCu_2MTe_4$ (M = Nb, Ta). The formal oxidation states of all atoms in this compound can be assigned as: Rb(+1), Cu(+1), Ta(+5), and Se(-2).

The compound $K_3Ag_3Ta_2Se_8$ (**4**) is, to the best of our knowledge, the first silver compound in the family with general composition $K_3M^I{}_3M^V{}_2Q_8$ (M^I = Cu, Ag; M^V = Nb, Ta; Q = S, Se). The main structural feature is a one-dimensional $[Ag_3Ta_2Se_8]^{3-}$ anionic

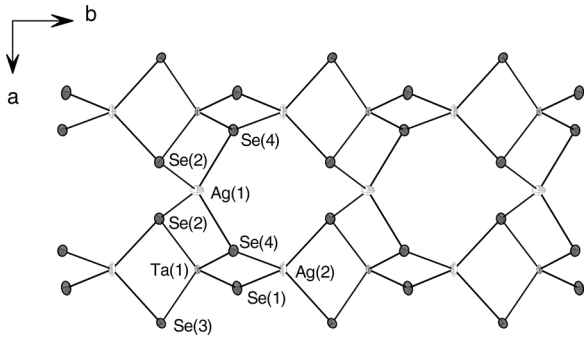

Fig. 5. Structure of $^1_\infty[Ag_3Ta_2Se_8]^{3-}$ anionic chain in compound **4** with labeling and displacement ellipsoids drawn at the 50% probability level.

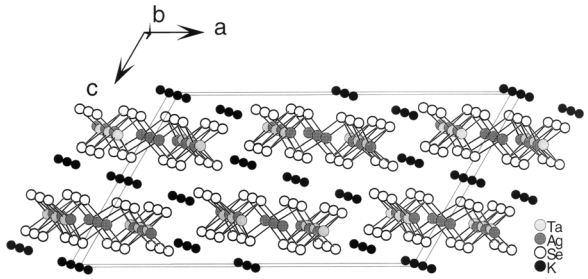

Fig. 6. Crystal structure of $K_3Ag_3Ta_2Se_8$ (**4**).

chain separated by K^+ ions (Fig. 5 and 6). The chains are directed along [010] with the shortest interchain separation of 3.748(1) Å between Se(2) atoms of adjacent chains. Within the chains the unique Ta atom and the two independent Ag atoms are tetrahedrally coordinated by Se atoms. The $TaSe_4$ and $Ag(2)Se_4$ tetrahedra share common edges along [100] to form infinite one-dimensional $[AgTaSe_4]$ chains which are topologically identical with those found in compounds **1** and **2**. Two adjacent chains are interconnected by $Ag(1)Se_4$ tetrahedra in such way that the $Ag(1)Se_4$ tetrahedra have common edges with $TaSe_4$ tetrahedra along [100] and common corners with $Ag(2)Se_4$ tetrahedra. Compared to compound **3**, the structure of **4** can be viewed as a derivative removing one half of the $Cu(1)Se_4$ tetrahedra from the two-dimensional layers in **3**. More precisely, the structure of the anionic chain is an intermediate between those in compounds **1**–**3**. Since there are no Se–Se interactions in this compound the formal oxidation states K(+1), Ag(+1), Ta(+5), and Se(-2) can be assigned. Similar copper – group 5 metal – chalcogen chains were found previously in $K_3Cu_3Nb_2S_8$ [19]. As expected, the Ta–Se and Ag–Se distances in compound **4** are longer

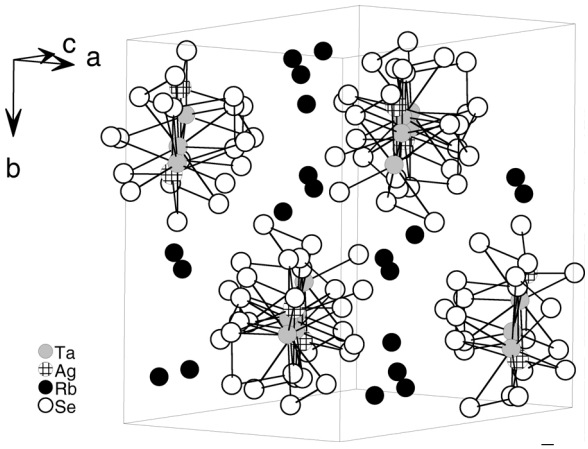

Fig. 7. Crystal structure of $Rb_3AgTa_2Se_{12}$ (**5**) along $[10\bar{1}]$.

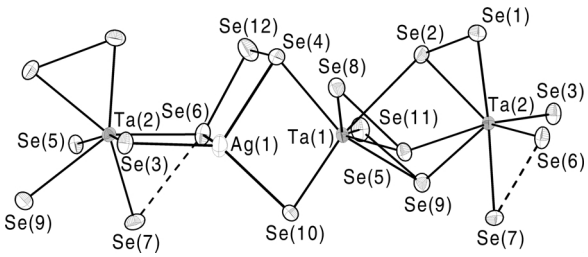

Fig. 8. Structure of the $^1_\infty[AgTa_2Se_{12}]^{3-}$ anionic chain in compound **5** with atomic labeling and displacement ellipsoid drawn at the 50% probability level (the dashed lines represent the long Se–Se distance of 2.838 Å).

than the analogous bonds in $K_3Cu_3Nb_2S_8$. The tetrahedra surrounding Ta, Ag(1), and Ag(2) are strongly distorted with the angles ranging from 104.81(3)° to 112.75(3)° for $TaSe_4$, 100.41(2)° to 121.30(5)° for $Ag(1)Se_4$, and 98.12(3)° to 121.64(3)° for $Ag(2)Se_4$, while in $K_3Cu_3Nb_2S_8$ the NbS_4 tetrahedra are somewhat more regular (107.98(7)°–112.27(7)°), $Cu(1)S_4$ (105.27(7)°–114.54(13)°), and $Cu(2)S_4$ (104.30(9)°–115.47(9)°).

The structure of $Rb_3AgTa_2Se_{12}$ (**5**) (Fig. 7 and 8) contains $[AgTa_2Se_{12}]^{3-}$ chains running along the $[10\bar{1}]$ direction with Rb^+ ions isolating these chains. In the structure, there are three independent Rb atoms. The Rb(1) ion is coordinated by nine Se atoms forming an irregular polyhedron whereas both Rb(2) and Rb(3) ions are coordinated to eight Se atoms. The Rb–Se distances range from 3.334(1) to 3.862(1) Å. In $K_3CuNb_2Se_{12}$ the coordination numbers of the K^+ ions are 10, 9, and 8.

Of particular interest in the structure of $Rb_3AgTa_2Se_{12}$ (**5**) is the fact that the two inde-

pendent Ta atoms are coordinated by seven Se atoms each forming a $TaSe_7$ pentagonal bipyramid. Two $TaSe_7$ polyhedra share a common face yielding a $[Ta_2Se_{11}]$ unit. We note that the Ta atoms are not in a tetrahedral environment as in compounds **1**–**4** and that the Se atoms form Se_3^{2-} species in **5**. The Ta(1) atom is surrounded by two Se_2^{2-} and two Se^{2-} anions and has a bond to a Se atom of the Se_2^{2-} dianion which is bound in a η^2-mode to Ta(2). In contrast, Ta(2) has bonds to one Se_2^{2-} anion, to three Se^{2-} ions and to one Se atom of the two Se_2^{2-} ions bound to Ta(1) in the η^2-mode. The coordination mode can be described as $[Ta_2(Se)_3(\mu_2\text{-}\eta^2, \eta^1\text{-}Se_2)_3(\mu_2\text{-}\eta^1, \eta^1\text{-}Se_3)]^{4-}$. Interestingly, the Se(7) atom is terminal and has no bonds to Ag^+ or Se^{2-}. We note that the connection mode within the $[Ta_2Se_{11}]$ unit in $Tl_4Ta_2Se_{11}$ is quite different and may be described as $[Ta_2(\mu\text{–}Se)(\mu\text{-}\eta^2, \eta^1\text{-}Se_2)_2(\eta^2\text{-}Se_2)_2(S\ e)_2]^{4-}$ [26].

Within the $[AgTa_2Se_{12}]^{3-}$ chain the $[Ta_2Se_{11}]$ units share edges with the $AgSe_4$ tetrahedra (Se(3)-Se(6) and Se(4)-Se(10)). The Se – Se distances in the Se_3^{2-} anion (Se(4)-Se(6)-Se(12)) range from 2.385(1) to 2.475(1) Å, typical values for single bonds. The Ta – Se bond lengths are between 2.421(1) and 2.931(1) Å, somewhat longer than the Nb – Se distances in $K_3CuNb_2Se_{12}$ [20]. The average distance $d_{Ta-Se} = 2.62$ Å is in good agreement with the sum of the ionic radii (Ta^{5+} (0.64 Å), Se^{2-} (1.98 Å)) [24]. It is also in agreement with the average distance ($d_{Ta-Se} \approx$ 2.61 Å) reported for $K_{12}Ta_6Se_{35}$ [25] and $Tl_4Ta_2Se_{11}$ [26]. But comparing compound **5** with $K_{12}Ta_6Se_{35}$ and $Tl_4Ta_2Se_{11}$ carefully, we found that the terminal Ta(2) – Se(7) distance (2.546(1) Å) is much longer than those in $K_{12}Ta_6Se_{35}$ (Ta – Se_{ter}: 2.360(1) – 2.376(1) Å) and $Tl_4Ta_2Se_{11}$ (Ta – Se_{ter}: 2.410(2) – 2.433(2) Å). Obviously, the Ta(2) – Se(7) bond cannot be described as a double bond. One reason for the elongation of the terminal Ta-Se(7) bond may be a weak interaction between Se(7) and Se(6) (see below).

The Ag – Se distances vary from 2.546(1) to 2.737(1) Å, comparing well with those in $RbAg_5Se_3$ (Ag – Se: 2.642(2) – 2.745(2) Å) [22], $RbAg_3Se_2$ (Ag – Se: 2.589(2) – 2.753(2) Å) [23] and those in compound **4** (2.629(1) and 2.676(1) Å). The $AgSe_4$ tetrahedron is strongly distorted with Se-Ag-Se angles ranging from 86.38(3)° to 126.81(3)°.

According to Lu and Ibers [20], the isostructural compound $K_3CuNb_2Se_{12}$ contains a Se_4^{2-} polyselenide anion with Se-Se distances between 2.389(3), 2.542(3), and 2.726(3) Å. In the present compound the comparable distances in compound **5** (Se(4)-Se(12)-Se(6)-Se(7)) amount to 2.400(1), 2.475(1), and 2.838(1) Å, the latter is much longer than a Se – Se single bond of about 2.35 Å. In addition, the Se(7) atom is only 3.028(1) Å apart from Se(9) and 3.011(1) Å from Se(5), and both separations are significantly shorter than the sum of the van der Waals radii of Se^{2-} anions. We note that in $K_3CuNb_2Se_{12}$ similar short contacts are observed (3.041 and 3.108 Å). The average Nb-Se bond length in the Nb compound is nearly identical with that observed in our compound. Hence, the structural differences within the anionic chains of the two compounds must be due to the differing bonding interactions and geometrical features in the $CuSe_4$ and $AgSe_4$ tetrahedra, respectively.

Vibrational spectroscopy

The FIR and Raman spectra of Rb_2CuTaS_4 (**1**) in the range of 80 to 475 cm^{-1} are shown in Fig. 9. The FIR spectrum displays absorptions at about 419, 407, 228, 208, 150, 140, 121, and 88 cm^{-1}. The Raman spectrum shows resonances at about 435, 422, 414, 251, and 170 cm^{-1}. Compared with the data of Cu_3TaS_4 and Tl_3TaS_4 [27], the Raman shifts at 435, 422, 414 cm^{-1} can be assigned to Ta – S (Cu – S) stretching vibrations. The resonance at 170 cm^{-1} is assignable to the S – Ta(Cu) – S deformation mode of the $Ta(Cu)S_4$ tetrahedra. Because all sulfur atoms are edge-shared by TaS_4 and CuS_4 tetrahedra, it is impossible to separate the Raman resonances of TaS_4 and CuS_4 tetrahedra exactly. Due to the somewhat shorter Ta – S and Cu – S bond lengths in compound **1**, these vibrations are located at higher energies. The shift at 251 cm^{-1} was attributed to the Cu – S valence vibration. The absorptions in the far-IR spectrum at 419, 407, 228, 208 cm^{-1} were assigned to Ta – S (Cu – S) asymmetric stretching vibrations. The assignments of the bands at a lower energy from 150 to 80 cm^{-1} are not clear.

Fig. 10 shows the FIR and Raman spectra of compound **4** in the range of 80 to 350 cm^{-1}. The FIR spectrum displays absorptions at about 277, 265, 248, 164, 140, 107, and 90 cm^{-1}, and the Raman spectrum shows resonances at about 287, 276, 268, 249, 156, 142, and 120 cm^{-1}. As a result of the lower site symmetry of the Ta, Ag(1), and Ag(2) atoms, the absorptions in the FIR and Raman spectra of compound **4** are splitted. On the basis of previous reports [27], the peaks

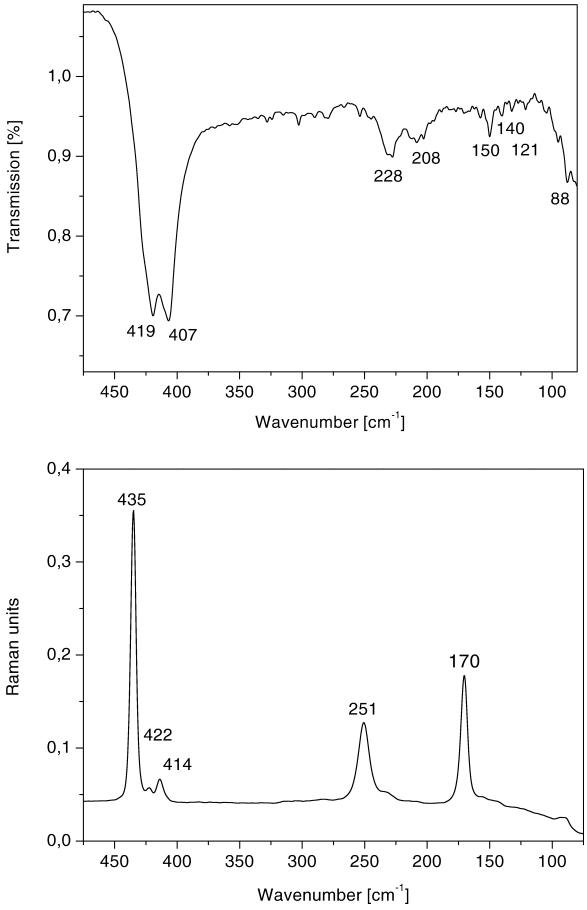

Fig. 9. FIR and Raman spectra of Rb_2CuTaS_4 (**1**) in the range of 80 to 500 cm^{-1}.

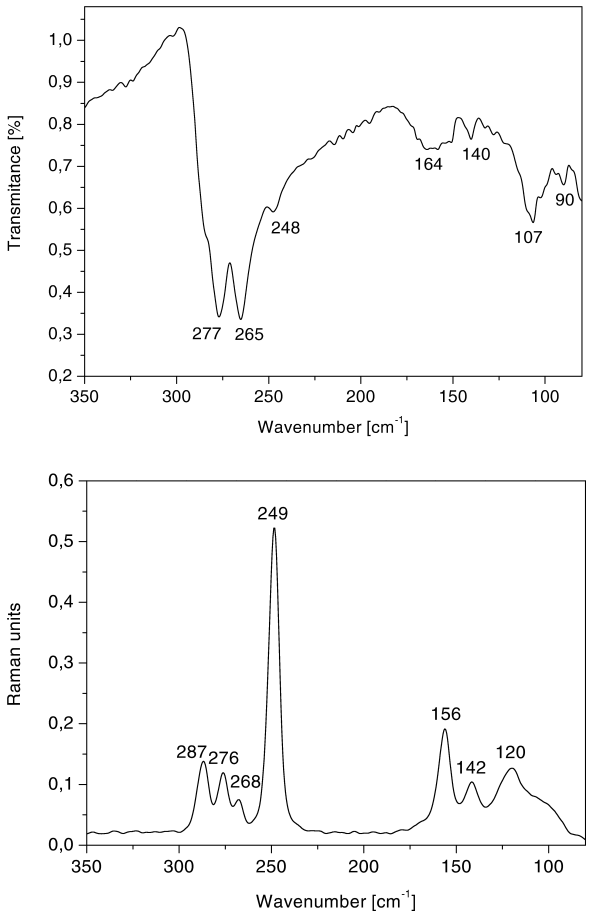

Fig. 10. FIR and Raman spectra of $K_3Ag_3Ta_2Se_8$ (**4**) in the range of 80 to 350 cm^{-1}.

in the Raman spectrum at 287, 268, and 249 cm^{-1} can be assigned to Ta(Ag)–Se symmetric stretching modes, the band at 276 cm^{-1} to an asymmetric vibration. The resonances at lower energies (200–100 cm^{-1}) may be assigned to the Ag–Se valence vibrations (156(ν_s) and 142 cm^{-1} (ν_{as})) and the Se–Ta(Ag)–Se deformation mode, respectively. The FIR spectrum is in good agreement with the Raman spectrum. Again the peaks at 277, 265, 248, 164, 140 cm^{-1} are due to Ta(Ag)–Se stretching modes, the absorptions at 107 and 90 cm^{-1} are assignable to deformation modes of Se–Ta(Ag)–Se and the unit cell vibration, respectively.

In conclusion, the five low-dimensional compounds Rb_2CuTaS_4, $Rb_2CuTaSe_4$, $RbCu_2TaSe_4$, $K_3Ag_3Ta_2Se_8$, and $Rb_3AgTa_2Se_{12}$ have been synthesized and characterized. The presence of different low-dimensional anions in these compounds obtained from a polychalcogenide flux suggests possible new phases formed by combinations of various polychalcogenide anions and different building units of Ta atoms.

Acknowledgements

Financial support by the State of Schleswig-Holstein and the Deutsche Forschungsgemeinschaft (DFG) is gratefully acknowledged.

[1] P. Dürichen, W. Bensch, Eur. J. Solid State Inorg. Chem. **33**, 309 (1996).
[2] C. Rumpf, R. Tillinski, C. Näther, P. Dürichen, I. Jess, W. Bensch, Eur. J. Solid State Inorg. Chem. **34**, 1187 (1997).
[3] W. Bensch, P. Dürichen, Chem. Ber. **129**, 1207 (1996).
[4] R. Tillinski, C. Rumpf, C. Näther, P. Dürichen, I. Jess, S. A. Schunk, W. Bensch, Z. Anorg. Allg. Chem. **624,** 1285 (1998).
[5] W. Bensch, P. Dürichen, C. Weidlich, Z. Kristallogr. **211**, 931 (1996).
[6] K. O. Klepp, G. Gabl, Eur. J. Solid State Inorg. Chem. **34**, 1119 (1997).
[7] Y.-J. Lu, J. A. Ibers, Inorg. Chem. **30**, 3317 (1991).
[8] W. Bensch, P. Dürichen, C. Weidlich, Z. Kristallogr. **211**, 932 (1996)
[9] Y. –J. Lu, P. Wu, J. A. Ibers, Eur. J. Solid State Inorg. Chem. **30**, 101 (1993).
[10] W. Bensch, P. Dürichen, C. Weidlich, Z. Kristallogr., **211**, 933 (1996).
[11] K. Peters, E.-M. Peters, H. G. von Schnering, C. Mujica, G. Carvajal, J. Llanos, Z. Kristallogr. **211**, 812 (1996).
[12] R. Tillinski, C. Näther, W. Bensch, Acta. Crystallogr. **C57**, 333 (2001).
[13] Y.-J. Lu, J. A. Ibers, J. Solid State Chem. **94**, 381 (1991).
[14] R. Tillinski, C. Näther, W. Bensch, Acta Crystallogr. **C55**, 1959 (1999).
[15] Y.-J. Lu, J. A. Ibers, J. Solid State Chem. **107**, 58 (1993).
[16] Y.-J. Lu, J. A. Ibers, J. Solid State Chem. **111**, 447 (1994).
[17] J. A. Cody, E. J. Wu, C. M. Cheung, J. A. Ibers, J. Solid State Chem. **121**, 225 (1996).
[18] J. Li, H.-Y. Guo, D. M. Proserpio, A. Sironi, J. Solid State Chem.**117**, 247 (1995).
[19] Y.-J. Lu, J. A. Ibers, J. Solid State Chem. **98**, 312 (1992).
[20] Y.-J. Lu, J. A. Ibers, Inorg. Chem. **30**, 3317 (1991).
[21] Bruker, Shelxtl Version 5.1, Bruker AXS Inc., Madison, Wisconsin, USA (1998).
[22] M. Emirdag, G. L. Schimek, W. T. Pennington, I. W. Kolis, J. Solid State Chem. **144**, 287 (1999).
[23] W. Bronger, J. Eyck, H. Schils, J. Less-Common Met. **60**, 5 (1978).
[24] R. D. Shannon, Acta Crystallogr. **A32**, 751 (1976).
[25] O. Tougait, J. A. Ibers, Solid State Sci. **1**, 523 (1999).
[26] Ch. L. Teske, N. Lehnert, W. Bensch, Z. Anorg. Allg. Chem. **628**, 2651 (2002).
[27] K. H. Schmidt, A. Müller, J. Bouwma, F. Jellinek, J. Mol. Struct. **11**, 275 (1972).